

Effects of carbon residue in atomic layer deposited HfO₂ films on their time-dependent dielectric breakdown reliability

Moonju Cho, Jeong Hwan Kim, and Cheol Seong Hwang^{a)}

Department of Materials Science and Engineering, Seoul National University, Seoul 151-742, Korea and Inter-university Semiconductor Research Center, Seoul National University, Seoul 151-742, Korea

Hyo-Shin Ahn and Seungwu Han^{b)}

Department of Physics and Division of Nano Science, Ewha Womans University, Seoul 120-750, Korea

Jeong Yeon Won

Analytical Engineering Center, Samsung Advanced Institute of Technology, P.O. Box 111, Suwon 440-600, Korea

(Received 13 March 2007; accepted 9 April 2007; published online 3 May 2007)

The effect of the carbon residue on the reliability of HfO₂ thin films was investigated. HfO₂ films were deposited on Si wafers by atomic layer deposition at a wafer temperature of 250 °C using Hf[N(CH₃)₂]₄ and O₃ oxidant with two different densities (160 and 390 g/m³). The films deposited at the higher O₃ density contained a lower concentration of carbon impurities. The leakage current density was lower and the time-dependent dielectric breakdown was improved in the higher O₃ density films. First principles calculations confirmed that trap sites were generated in the band gap of HfO₂ when carbon was interstitially or substitutionally present. © 2007 American Institute of Physics. [DOI: 10.1063/1.2735945]

Hafnium oxide (HfO₂) thin films have been extensively studied as the gate dielectric for semiconductor logic devices, due to their superior gate leakage current characteristic compared to that of SiO₂.¹⁻⁴ Although the gate leakage current could be almost 10⁶ times smaller compared to SiO₂, the carrier mobility and reliability degradation in HfO₂ is still a serious problem⁵⁻⁷ due to the high density of traps in the HfO₂ film. In the deposition process of HfO₂ films by atomic layer deposition (ALD) using HfCl₄ or metal-organic Hf precursors, such as Hf[N(CH₃)₂]₄ used in this study, contamination of the film by Cl or C appears to be inevitable. Cho *et al.* recently reported that the Cl residue in ALD HfO₂ films does not influence their reliability and dielectric performances.⁸ Although the influence of the C residue in SiO₂ gate dielectrics on their reliability has been studied by several groups, few similar studies of HfO₂ have been reported. Bersuker *et al.*⁹ showed the effect of carbon on the time-dependent dielectric breakdown (TDDB) reliability of SiO₂ films. They implanted four different doses of carbon (0, 1 × 10¹³, 1 × 10¹⁴, and 5 × 10¹⁴ atoms/cm², implantation energy of 10 keV) into the Si substrate through a 15 nm sacrificial oxide layer. It was clearly observed that a lower carbon dose improved the TDDB of SiO₂. Triyoso *et al.*¹⁰ compared the leakage current characteristics of ALD HfO₂ films deposited with HfCl₄ and H₂O containing Cl residue at a concentration of 7 × 10¹³ atoms/cm² and metal-organic chemical vapor deposited (MOCVD) HfO₂ films with Hf-*t*-butoxide Hf(C₄H₉O)₄ and NO containing carbon residue at a concentration of 1.4 × 10¹³ atoms/cm². They found that the MOCVD HfO₂ films showed a higher leakage current density even at a thicker capacitance equivalent oxide thickness (CET), due to the trap-related electrical conduction in the MOCVD HfO₂. However, they did not report the reliability

properties of the HfO₂ films as a function of the carbon residue content. Therefore, in this study, the influence of the carbon residue on the leakage current and reliability of ALD HfO₂ films grown using Hf MO precursor and O₃ with two different O₃ densities was evaluated. When the higher O₃ density was used, HfO₂ films with a lower carbon-residue content were obtained and vice versa. In order to confirm the relationship of the leakage and reliability properties to the amount of carbon residue, the energy band structure of HfO₂ was calculated using first principles calculations when C atoms were present in the HfO₂ films.

HfO₂ films were deposited using an 8 in. diameter scale traveling-wave-type ALD reactor (Quoros Co., Plus 200). The native oxide on the Si wafer surface was removed by a RCA-cleaning process prior to the deposition of the film. The Hf[N(CH₃)₂]₄ precursor and O₃ pulse durations were 2 and 3 s, and Ar purge gas was injected for 9 and 3 s after each of these two chemical pulses, respectively. The deposition temperature was set to 250 °C. Details of the ALD process have been previously reported.³ O₃ oxidant with two different densities (160 and 390 g/m²) was used to deposit HfO₂ films with different carbon-residue contents. The HfO₂ samples grown with the low and high densities of O₃ are referred to as H-l and H-h, respectively. The postdeposition annealing (PDA) was performed using a rapid thermal processing system at temperatures ranging from 600 to 1000 °C for 30 s in a flowing pure N₂ atmosphere to test the thermal stability of the films. Electron beam evaporated platinum was deposited as the top electrode after the PDA. Subsequently forming gas annealing was performed at 400 °C for 30 min under a 95% N₂/5% H₂ atmosphere. The film thickness was measured by a single wavelength ellipsometer which was calibrated by high-resolution transmission electron microscopy. The depth profiles of the chemical composition of the film stacks were investigated by time-of-flight secondary ion mass spectroscopy (ToF-SIMS). The capacitance-voltage (*C-V*), leakage current-voltage (*J-V*), and flatband voltage shift characteris-

^{a)}Electronic mail: cheolsh@snu.ac.kr

^{b)}Electronic mail: hansw@ewha.ac.kr

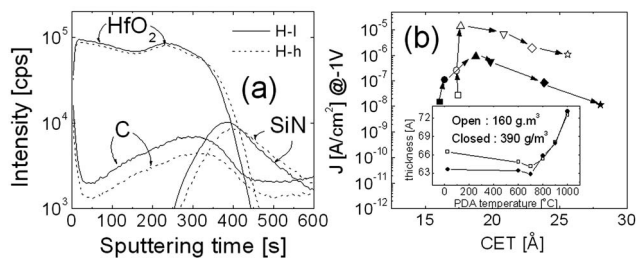


FIG. 1. (a) C, HfO₂, and SiN depth profiles of the as-deposited H-h and H-l samples by ToF-SIMS, (b) plot of J vs CET of the H-h and H-l samples before and after PDA at temperatures ranging from 600 to 1000 °C. The inset figure in (b) shows the variations in film thickness as a function of the PDA temperature.

tics of the metal-insulator-semiconductor capacitors were investigated using an HP 4194 impedance analyzer and HP 4140B picoammeter/dc voltage source. The capacitance equivalent thickness (CET) was calculated from the accumulation capacitance at 1 MHz. The time to breakdown (t_{BD}) and time-dependent dielectric breakdown characteristics were measured under the gate injection condition (negative bias on Pt gate) with the constant voltage stress (CVS) method.

Figure 1(a) shows the C, HfO₂, and SiN intensity profiles of the two as-grown samples analyzed by ToF-SIMS. The peak carbon intensity of sample H-l is ~ 1.6 times higher than that of sample H-h. The absolute concentration of carbon atoms in the film is unknown, due to the lack of proper standards for the quantification of carbon in HfO₂ for this tool. PDA at temperatures >700 °C generally decreases the carbon density in the HfO₂ film, but increases it at the film/substrate interface (data not shown). It has been reported that a thin SiN layer was formed at the interface during ALD using the Hf[N(CH₃)₂]₄ precursor and that the SiN layer acted as an effective reaction barrier layer between the HfO₂ film and Si substrate, which resulted in improved thermal stability and interface trap properties.³ The comparison between the locations of the peak positions of the C, HfO₂, and SiN signals shows that the carbon residue exists inside the HfO₂ layer, although the peak position is located near the interface. If the C atoms act as charge traps inside the HfO₂ film, this location of the C peak suggests that the C atoms are harmful to the device operation, since the carriers in the channel region can be easily trapped by quantum-mechanical tunneling through the thin SiON interface layer. Therefore, lowering the C-residue content by adopting a high O₃ density could be crucial.

Figure 1(b) shows the J (measured at -1 V) vs CET plot of the two samples before (square symbol) and after the PDA at 600 (circle symbol), 700 (up triangle symbol), 800 (down triangle symbol), 900 (diamond symbol), and 1000 (star symbol) °C. The arrows indicate the direction of the variation with increasing PDA temperature. The authors previously reported the variations in the CET and interface trap density as a function of the PDA temperature for samples grown with different O₃ densities.¹¹ The HfO₂ films grown by the present ALD process are oxygen excessive (O/Hf atomic ratio = 2.1–2.2 by the x-ray photoelectron spectroscopy depending on the O₃ density) and the degree of oxygen excess decreases with decreasing O₃ density during the deposition. Therefore, a lower O₃ density resulted in a smaller increase in the CET due to the less serious interfacial

oxidation.¹¹ This is also observed in the present study, as shown in Fig. 1(b). The CET of sample H-h increases from 16 Å in the as-deposited state to 28 Å after the PDA at 1000 °C, whereas that of sample H-l increases from 17.5 to 25.5 Å after the same PDA. Especially, the increase in CET of sample H-l is negligible up to 700 °C. However, the leakage current behavior shows the opposite trend; with increasing PDA temperature, J of sample H-l degrades much further than that of sample H-h. The fast increase in J up to the PDA temperature of 700 °C is due to the crystallization of the HfO₂ films and decrease in film thickness by densification [inset in Fig. 1(b)] without any significant interfacial layer growth. As the PDA temperature increases above 800 °C, the significant growth of the interfacial layer causes J to decrease with increasing PDA temperature. The higher carbon-residue content of sample H-l might be the reason for the higher value of J for all PDA conditions. As discussed below, by using the first principles calculation results, carbon, which is interstitially present in the HfO₂ film, forms a deep trap level (~ 0.8 eV from the conduction band edge) in the band gap, and thus provides a leakage path by trap assisted tunneling or Poole-Frenkel mechanisms.

In order to determine the microscopic origin of the observed increases in the trap site density, first principles calculations were carried out on the carbon defects embedded in the HfO₂ films.^{12,13} Two types of doping, substitutional and interstitial, are considered as the possible defect forms of carbon. To be compatible with the periodic boundary condition, $2 \times 2 \times 2$ supercells formed by expanding the original monoclinic HfO₂ were used and various initial positions were tried for the C atoms. The energy cutoff was set to 500 eV and a $2 \times 2 \times 2$ k -point mesh was used for the integration in the first Brillouin zone. All of the atomic positions were relaxed until the Hellmann-Feynman force on each atom was reduced to within 0.05 eV/Å.

There are two types of oxygen atoms in the monoclinic phase of the HfO₂ film, having threefold (O3) and fourfold (O4) coordination with the nearby Hf atoms, respectively. For interstitial defects, the minimum energy is found when the carbon atom is placed in a large void between the O3 and O4 layers. The final geometry indicates that the carbon atom is attached to O4 with a bond length of 1.35 Å [see Fig. 2(a)]. On the other hand, for substitutional defects, the carbon atom is most stable when replacing O4 [see Fig. 2(b)]. In this case, the relaxation of the surrounding atoms is very small, since the atomic size of the carbon atom is similar to that of the oxygen atom. From the analysis of the defect formation energy, it was found that the interstitial defect is favored under the oxygen-rich growth condition, while the substitutional form is more stable near the metal-rich limits. On the right-hand side of Fig. 2, the total and partial densities of states are shown for both defect arrangements. The partial densities of states are obtained by projecting the wave functions onto the carbon atoms. In both cases, it was found that the carbon atoms induce two localized states within the energy gap. Further analysis shows that they are mainly composed of C- p orbitals as well as Hf- d and O- p orbitals close to the defect site. The presence of localized levels due to the carbon atoms is in good agreement with the experimental observation of the increased leakage current of sample H-h. The oxygen excess composition of the present samples (O/Hf ratio ~ 2.1 – 2.2) favors the interstitial model of carbon atoms, and thus the main defects that contributed to the

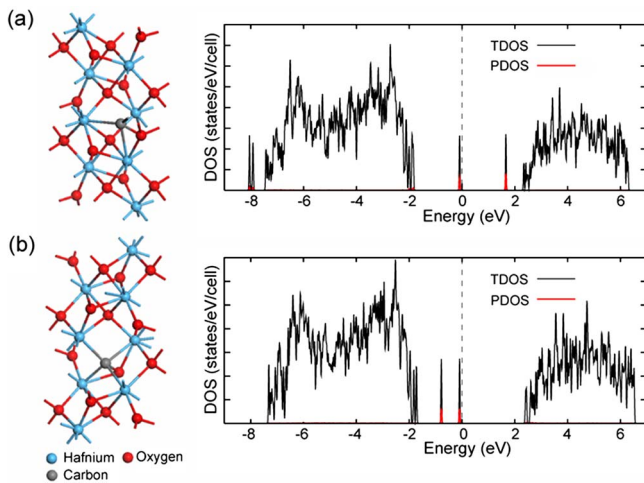


FIG. 2. (Color online) Relaxed atomic structure around the carbon defects in monoclinic HfO_2 . (a) The interstitial and (b) substitutional carbon defects. The corresponding total and partial densities of states are shown on the right-hand side.

electrical conduction are the deep acceptor (~ 0.8 eV from the conduction band edge) levels shown in the upper panel of Fig. 2.

In order to determine the effect of the carbon residue on the reliability, the TDDDB was evaluated in the as-deposited H-h and H-l samples at room temperature. CVS was applied at -4.3 , -4.35 , and -4.6 V in the H-l; and -4.3 and -4.6 V in the H-h samples. Both of these samples show hard breakdown behavior, as shown in the inset of Fig. 3(b). The initial current was higher for sample H-l than for sample H-h. It was also higher when the CVS voltage was higher in both samples. These initial current density trends are consistent with the J vs CET data shown in Fig. 1(b) and the J - V curves (data not shown). t_{BD} was collected and analyzed by means of a Weibull plot, as shown in Fig. 3(a). t_{BD} was shorter under harsher CVS conditions and was longer in sample H-h than in sample H-l for the given CVS condition. Degraeve *et al.* recently suggested a model for the hard breakdown of HfO_2 film based on a formation of a “percolation path” caused by the electrical stress.¹⁴ Kyuno *et al.* recently reported the presence of localized current paths in thin HfO_2 films using conductive atomic force microscopy.¹⁵

Because carbon atoms form trap levels inside the band gap, they can form a permanently conducting path once they percolate. However, it is not known if the carbon atoms can

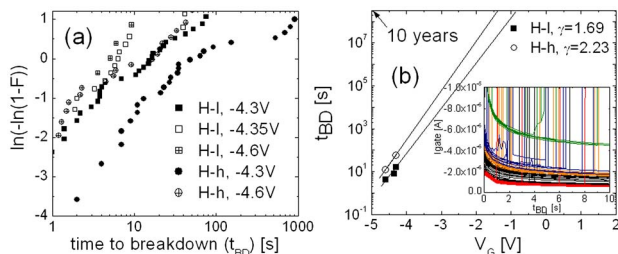


FIG. 3. (Color online) (a) Weibull distribution from TDDDB analysis in as-deposited H-h and H-l samples. (b) Lifetime extrapolation from the Weibull distribution in (a) by log-linear plot. The inset shows the J -time plots under the various CVS voltages.

migrate easily inside the HfO_2 film in the presence of an applied field at room temperature. Although the nature of the percolation path is not known, the presence of a high density of carbon residue certainly promotes the breakdown caused by the larger leakage current before the breakdown actually occurs. The high current density may enhance the electromigration of the defects that would form the percolation paths and the Joule-heating effect also contributes to the migration of defects. The lifetime was evaluated as shown in Fig. 3(b) in log-linear form. Sample H-h guarantees a lifetime >10 yr under the -1.0 V operation condition, whereas sample H-l shows a lifetime of 10 yr only at voltages $< \sim -0.8$ V.

In summary, the effects of the carbon residue on the leakage current and reliability properties of ALD HfO_2 thin films were investigated. The use of a high and low density of O_3 during the ALD of HfO_2 resulted in the formation of HfO_2 films with low and high densities of carbon residue, respectively. Although sample H-l exhibited better thermal stability of the CET with increasing PDA temperature, its overall J vs CET performance was inferior to that of sample H-h, due to its higher leakage current for all conditions. The first principles calculations showed that the interstitial carbon atoms in the HfO_2 films produced deep acceptorlike trap states in the band gap, which may enhance the electrical conduction by a trap-mediated conduction mechanism. Accordingly, the 10 yr lifetime of sample H-h was guaranteed at -1 V, whereas that of sample H-l was only obtained at voltages lower than -0.8 V.

This work was supported by the system IC 2010 project of the Korean government.

- ¹A. Delabie, M. Caymax, B. Brijs, D. P. Brunco, T. Conard, E. Slesckx, S. V. Elshocht, L.-Å. Ragnarsson, S. De Gendt, and M. M. Heyns, *J. Electrochem. Soc.* **153**, F180 (2006).
- ²M. S. Akbar, N. Moumen, J. Barnett, J. Sim, and J. C. Lee, *Appl. Phys. Lett.* **86**, 032906 (2005).
- ³M. Cho, J. Park, H. B. Park, S. W. Lee, T. J. Park, C. S. Hwang, G. H. Jang, and J. Jeong, *Appl. Phys. Lett.* **85**, 5953 (2004).
- ⁴Y.-C. Yeo, T.-J. King, and C. Hu, *Appl. Phys. Lett.* **81**, 2091 (2002).
- ⁵A. Kerber, E. Cartier, L. Pantisano, R. Degraeve, T. Kauerauf, Y. Kim, A. Hou, G. Groeseneken, H. E. Maes, and U. Schwalke, *IEEE Electron Device Lett.* **24**, 87 (2003).
- ⁶L. Militaru, O. Weber, M. Muller, F. Ducroquet, D. Duscic, C. Plossul, T. Emst, B. Guillaumot, S. Deleonibus, and T. Skotnicki, *Proceeding of the 34th European Solid-State Device Research Conference*, 21 September 2004, p. 181.
- ⁷M. S. Akbar, J. C. Lee, N. Moumen, and J. Peterson, *Appl. Phys. Lett.* **88**, 082901 (2006).
- ⁸M. Cho, R. Degraeve, G. Pourtois, A. Delabie, L.-A. Ragnarsson, T. Kauerauf, G. Groeseneken, S. D. Gendt, M. Heyns, and C. S. Hwang, *IEEE Trans. Electron Devices* **54**, 752 (2007).
- ⁹G. Bersuker, J. Guan, G. Gale, P. Lysaght, D. Riley, and H. R. Huff, *IEEE Integrated Reliability Workshop Final Report*, 21 October 2002, p. 29.
- ¹⁰D. H. Triyoso, M. Ramon, R. I. Hegde, D. Roan, R. Garcia, J. Baker, X.-D. Wang, P. Fejes, B. E. White, Jr., and P. J. Tobina, *J. Electrochem. Soc.* **152**, G203 (2005).
- ¹¹J. Park, M. Cho, S. K. Kim, T. Park, S. W. Lee, S. H. Hong, and C. S. Hwang, *Appl. Phys. Lett.* **86**, 112907 (2005).
- ¹²G. Kresse and J. Hafner, *Phys. Rev. B* **47**, 558(R) (1993); **49**, 14251 (1994).
- ¹³D. M. Ceperley and B. J. Alder, *Phys. Rev. Lett.* **45**, 566 (1980).
- ¹⁴R. Degraeve, A. Kerber, Ph. Roussel, E. Cartier, T. Kauerauf, L. Pantisano, and G. Groeseneken, *Tech. Dig. - Int. Electron Devices Meet.* **2003**, 935.
- ¹⁵K. Kyuno, K. Kita, and A. Toriumi, *Appl. Phys. Lett.* **86**, 063510 (2005).